Identification of Human Immunodeficiency Virus Type 1 (HIV-1) Based Virus-Like Particles by Multifrequency Atomic Force Microscopy.

González-Domínguez I, Gutiérrez-Granados S, Cervera L, Gòdia F, Domingo N.

KEYWORDS:

Virus-like particle (VLP), Atomic Force Microscopy (AFM), Multifrequency AFM, Bimodal AFM, AM-FM Viscoelastic Mapping Mode, Human Immunodeficiency Virus (HIV)

ABSTRACT:

Virus-like particles (VLPs) have become a promising platform for vaccine production. VLPs are formed by structural viral proteins that inherently self-assemble when expressed in a host cell. They represent a highly immunogenic and safe vaccine platform, due to the absence of the viral genome and its high protein density. One of the main important parameters in vaccine production is the quality of the product. A related bottleneck in VLP-based trials is the presence of cellular vesicles as a major contaminant in the preparations. Therefore, it is highly required the set up of techniques that allow for specific discrimination of VLPs from host vesicular bodies. In this work, novel Multifrecuency Atomic Force Microscopy (MF AFM) has permitted full structural nanophysical characterization by its access to the virus capsid of the HIV based VLPs. The assessment of these particles by advanced Amplitude Modulation-Frequency Modulation (AM-FM) Viscoelastic Mapping mode has enhanced the imaging resolution of their nanomechanical properties opening a new window for the study of the biophysical attributes of VLPs. Finally, the identification and differentiation of HIV based VLPs from cellular vesicles has been performed under ambient conditions providing a novel methodology for the monitoring and quality control of VLPs.

1. INTRODUCTION

Currently, more than 37 million people worldwide are living with the human immunodeficiency virus (HIV) and the epidemic still has a substantial effect on certain countries and high-risk groups (1). Despite several efforts have been undertaken to find a proper vaccine, there is no current effective candidate against HIV infection (2). HIV is an enveloped single-stranded RNA virus whose genome gives rise to three main polyproteins: Gag, Gag-Pol and Env. Gag gene contains the main structural proteins of HIV. Upon expression, Gag polyprotein is able to self-assemble generating non-infectious virus-like particles (VLPs) that have shown great promise as a platform for the presentation of antigens (3).

VLP-based vaccine candidates for HIV have satisfactorily been produced in mammalian and insect cells (4, 5). VLPs display a high protein density on their surface. Moreover, they represent a highly immunogenic and safe vaccine system compared to other third generation vaccines, since they do not contain the viral genome (4–6). In this study, HIV-1 Gag-based VLPs produced by transient gene expression in mammalian cells following the previously described methodology are examined (7, 8).

Similar to the native HIV virus, HIV-1 Gag VLPs are released by the cell through a budding process after the Gag polyprotein self-assembly. Thus, the final particles are enveloped by the host cell lipid membrane (3). Additionally, the cell machinery also naturally secretes other cellular vesicles to the extracellular space such as microvesicles and exosomes (9). The presence of these cellular vesicles has been previously described in HIV and Influenza-based VLPs produced in mammalian cells (10–12) and it has also been observed in our research laboratory in all HIV-1 based VLP preparations. The need for high quality VLP-based vaccine productions is prevailing since its end-use is their human clinical application (6).

Nowadays, there are not proper techniques which allow specific discrimination of VLPs from cellular vesicles, hence the presence of vesicular bodies becomes a major bottleneck in the field of VLP-based vaccine production trials. For this reason, the characterization of both HIV-1 Gag VLPs and cellular vesicles is of high relevance with a view to the further development of purification methods. These particles have been previously characterized by Electron Microscopy (EM) (7, 13). However, EM analysis requires a negative staining pre-treatment which can lead to false positive errors and also lacks tridimensional structural information. Further evaluation is essential to understand the morphology and mechanical attributes of the product.

In this work, Atomic Force Microscopy (AFM) is proposed for investigating the HIV-1 Gag VLP population. AFM has been already used in virus and VLP characterization providing novel information of biological samples, such as morphology, structural data and composition in ambient conditions (14–16). Interestingly, recent advances in multifrequency (MF) AFM modes offer a broad assessment of nanomechanical features of soft samples. The dynamic mechanical properties of an AFM cantilever are composed by a set of eigenmodes associated to different resonant frequencies. MF AFM exploits the simultaneous excitation and/or analysis of different eigenmodes and harmonics in the deflection signal to enhance the information about the tip-sample interactions. Thus, this MF AFM technique deepens into the material characteristics. Of note the application of MF AFM modes, such as amplitude modulation-frequency modulation (AM-FM) Viscoelastic Mapping, to soft samples characterization (17, 18).

In this study, the application of AM-FM Viscoelastic Mapping to analyze enveloped VLPs is reported for the first time, with the obtention of interesting new data of its composition and internal capsid protein structure. HIV-1 Gag VLPs were analyzed by MF AFM and its use facilitated the discrimination between VLPs and cellular vesicles present in the preparations. Nonetheless, the sample preparation based on EM protocol has important drawbacks due to the alteration of the sample and the difficulties of working with grids in AFM. For these reasons, the VLP samples were also examined under ambient conditions deposited on mica substrate. In this simple configuration, we have validated an innovative and nimble methodology for discriminating VLPs and cellular vesicles under ambient conditions.

2.MATERIALS AND METHODS

2.1. HIV-1 Gag VLP production and purification

HIV-1 Gag VLPs were produced and purified by transient transfection protocol previously described (7, 13) in the human cell line: HEK 293SF-3F6 cells (kindly provided by Dr. Amine Kamen at the McGill University, Montreal, Canada). Gag gene was fused to GFP for its study, and preparations were quantified by an spectrofluorometric assay (13). A transfection with an empty plasmid was performed as a negative control (Mock).

2.2. HIV-1 Gag VLP Sample preparation for AFM and EM analysis

HIV-1 Gag VLPs samples were prepared by two different protocols as described below.

2.2.1. Negative staining in carbon coated grids

HIV-1 Gag VLP and Mock samples were diluted 1:4 with PBS, and subsequently negatively stained at Servei de Micròscopia (UAB, Bellaterra, Spain). Briefly, 5 µL of the preparation was deposited on Quantifoil gold-coated grids (QUANTIFOIL ® R2/2, Großlöbichau, Germany) and carbon-coated grids (PELCO® Center-Marked Grids, Redding, Canada) and incubated at room temperature for 5 minutes. Excess sample was carefully drained off the grid with the aid of filter paper. Then, samples were stained with 5 µL of uranyl acetate (2%) by incubating for 1 minute at room temperature. Excess staining was dried off as explained before and grids were dried for a minimum of 50 minutes at room temperature before examination.

2.2.2. VLP preparation by deposition on mica substrate

Mica substrate was prepared by defoliation prior to depositing 20 µL of VLP preparations. Samples were incubated during 15 minutes at room temperature. Afterwards, the sample was washed with 3 mL of MiliQ water. Finally, samples were dried with a gentle flow of nitrogen gas.

2.3. EM analysis

EM analysis was performed by two different microscopes. Transmission Electron Microscopy (TEM) examination was performed with JEM-400 (Jeol, California, USA) transmission electron microscope equipped with a Gatan ES1000W Erlangshen CCD Camera (Model 785). Scanning electron microscopy (SEM) images were assessed with FE-SEM Merlin (Zeiss, Jena, Germany) scanning electron microscope.

2.4. AFM analysis

Atomic Force Microscopy imaging was performed with a MFP-3D Asylum AFM (Oxford Instruments, California, USA). In all the experiments, PPP-EFM tips (Nanosensors TM, Schaffhausen, Switzerland) with a stiffness constant k = 2 N/m and coated with Ptlr5 were used. MF AFM is based in the use of multiple excitation modes with different characteristic frequencies. In this case, the fundamental excitation mode was used together with the second eigenmode. In simple Bimodal AFM operation mode, the tip is excited at both frequencies, with amplitudes A2<A1. A remarkable benefit of multifrequency bimodal imaging is the fact that the forces between the tip and the sample are very small while allowing a clear non-destructive differentiation of composition, which makes it very convenient to investigate soft biological samples. The excitation at the fundamental mode was used to measure the topography in Amplitude Modulation AFM (AM-AFM), while changes in amplitude and phase for the second eigenmode, not affected by the feedback loop restrictions, are monitored.

On the other hand, AM-FM Viscoelastic Mapping®operation mode of Asylum Research (Oxford Instruments, California, USA) was used to obtain direct contrast from mechanical properties of the samples. Similar to Bimodal AFM, two cantilever resonances are operated simultaneously; the fundamental mode was used for AM topography imaging, while a higher resonance mode is operated in FM, with an automatic gain control circuit monitoring the amplitude at the resonance frequency and adjusting the drive voltage to keep the amplitude constant, thus measuring the associated dissipation. The resonance frequency shifts describe the changes in elastic tip-sample interaction, and quantitative nanomechanical information can be obtained from analysis of the amplitude (A) and phase (Φ) of the two modes, together with the frequency and the dissipation at the second eigenmode. Detailed quantitative nanomechanical analysis can be performed on the base of the application of the Virial and energy transfer expressions among the multiple excited modes. Exact equations canb e found in the work by R. Garcia and R.Proksch [ref A, B]. The different features of each MF AFM operation mode are presented in table 1.

ModeName	Feedbackmode 1	Feedbackmode 2	Observables	Material property
Bimodal AFM	AM	Open	A_1, A_2,Φ_1, Φ_2	Dissipation
AM-FM Viscoelastic Mapping	AM	Frequency Modulation	A_1, Φ_1, Dissipation$_2$, Δf_2	Dissipation, Stiffness, Young modulus (E)

* A_n: Amplitude, Δf_n: Frequency shift, Φ_n: Phase

Table 1: Description of the two different working modes of MF AFM used in this work.

3. RESULTS AND DISCUSION

3.1. Characterization of HIV-1 Gag VLPs and cellular vesicles by EM

HIV-1 Gag VLPs and Mock samples were produced and analyzed by EM techniques. Figure 1A shows a TEM image of the vaccine candidate preparation. The particles are visualized as circular-like constructs of around 150 nm formed by electrodense material inside, corresponding to the Gag assembled capsid, enveloped by a lipid membrane observed as a bright corona. A second population of cellular vesicles is also detected in all VLP samples. The presence of cellular debris has also been reported in Influenza-based VLP produced in mammalian cells (12). Cellular vesicles are heterogeneous in size and present liposome-like circular structure. No electrodense contrast is spotted when its internal content is examined, which means they do not contain structured proteins as those present in VLPs. These vesicular bodies are characteristic of Mock samples (data not shown) where no HIV-1 Gag VLPs structures were recognized.

Figure 1: Electron Microscopy Analysis of HIV-1 Gag VLP preparations. (A)Transmission Electron Analysis of HIV-1 Gag VLPs (B) Scanning Electron Microscopy Analysis deposited on carbon-coated grids. Straight blue arrows point to HIV-1Gag VLPs and red dash arrows indicate cellular vesicles structures.

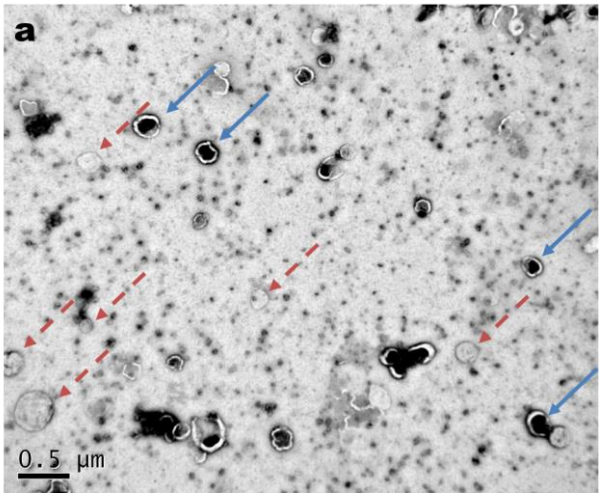

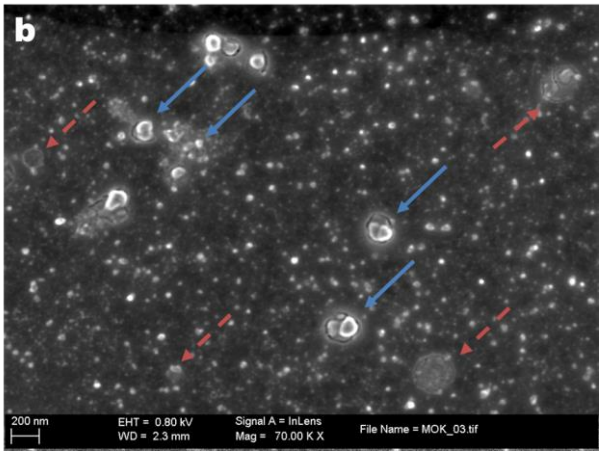

Figure 1B shows a SEM image of HIV-1 Gag VLP preparation. The particles are observed as sphere-like structures of 150 nm as those obtained in Figure 1A. Interestingly, the vesicular contamination is regarded as flatten circular structures. SEM analysis allow to infer that cellular vesicles lose their morphology during the negative staining protocol while HIV-1 Gag VLPs maintain their conformation. The different characteristics in front of negative staining can be caused by the presence of the protein capsid inside the vaccine candidate. Hence, the protein capsid offers higher mechanical resistance to these particles compared to the cellular vesicles.

The difference between the HIV-1 Gag VLPs and the vesicular population represents a potential opportunity to develop a proper purification protocol for VLPs. However, the study of biological material by EM requires the sample to be placed in vacuum conditions. Moreover, the imaging contrast obtained by TEM depends on the electrodensity of the sample and SEM examination needs the specimen to be conductive, requiring the coating and drying of biological materials in both cases. Additionally, negative staining treatment can lead to false positive errors due to the fact that uranyle acetate deposition is not completely homogenous and VLP-like structures can be confused with a nanometric accumulation of uranyle acetate. Altogether, the application of EM techniques for regular HIV-1 Gag VLP detection in quality control analysis is limited.

3.2 Identification of HIV-1 Gag VLP by AFM

Individual HIV-1 Gag VLP identified in TEM sample was further characterized by AFM to delve into the mechanical properties of the VLPs.

Figure 2A shows the VLP examined by TEM and in Figure 2B-D the results of the Air Dry non-contact AFM investigation of the topography, amplitude (A_1) and phase charts (Φ_1) are depicted, respectively. While TEM gives information about the internal content on the basis of electrodensity contrast, AFM provides detailed data of the HIV-1 Gag VLP morphology. HIV-1 Gag VLP topography AFM analysis (Figure 2B) presents a height of around 90 nm and a diameter of around 250 nm. The higher diameter compared with TEM data can be explained due to the tip convolution effect (16). When HIV-1 Gag VLP diameter is calculated in the mean height as performed by Faivre-Moskalenko (15), a diameter of around 150 nm is obtained, which is in agreement with previous measurements performed with TEM. Nonetheless, the determination of the particle size for this sample is affected by the adsorption effect of VLPs into the substrate, hindering the determination of the real particle size by AFM (14).

No relevant roughness was detected in the surface HIV-1 Gag VLP structures (Figure 2B). Kuznetsov *et al.*(19) analyzed wild HIV-1 viruses by dynamic AFM and gp40 glycoprotein was identified at the surface of the virus in contrast with the observation present in this study. Even so, the absence of surface protein is explained as the HIV-1 Gag VLPs produced in this work are only formed by the Gag gene and HIV-1 glycoproteins are contained in the Env region of the viral genome.

Of note, a significant contrast in the surface of the particle which is not related to topography data is observed in the Φ_1 image (Figure 2D). Phase contrast in AM images is related to dissipative processes hinting at the mechanic-physical properties of HIV-1 Gag VLPs, for which advanced MF AFM modes were applied to deepen into the nanomechanical qualities of the samples.

3.3. Advanced characterization of HIV-1 Gag VLP by MF AFM

As previously discussed, MF AFM involves techniques where cantilever motion is driven and measured at multiple frequencies. Advanced bimodal AFM (Figure 2E-F) and AM-FM Viscoelastic Mapping (Figure 2G-H) were applied to characterize the HIV-1 Gag VLP.

Figure 2E-F shows the amplitude (A_2) and phase (Φ_2) of the second resonance frequency as measured by Bimodal AFM. These images were taken under the following parameters: initial free oscillating amplitude of the fundamental mode A_{01} = 92.5 nm, setpoint amplitude for topography image recording of A_{sp}= 71 nm, and free oscillating amplitude at the second mode A_{02} = 5.5 nm, corresponding to a ratio A_{02}/A_{01} ~ 6%. The value of the first resonance frequency was f_1 = 80.21 kHz and f_2 = 501.84 kHz, with a relationship of f2/f1 ~6.25, which is adecuated for the correct application of bimodal imaging theory for this type of tips [ref C]. As demonstrated by simulations by Damircheli et al., [ref D] phase contrast in bimodal AFM strongly depends on the relationship between the free amplitudes of the two excited modes: substantial improvement of the contrast in bimodal AFM appears when the free amplitude of the second resonant mode is minimized. Good phase constrast of the second resonant mode in both, attractive and repulsive regimes, is achieved with relationships of $A_{02}/A_{01} < 1/10$, being almost maximum for relationships close to A_{02}/A_{01} ~ 1/20. In our case, the origin of the strong phase contrast observed can be explained by the appropriate chosen relationship of our working amplitudes which is about A_{02}/A_{01} ~ 1/17. The enhanced contrast in bimodal AFM images of the internal structure perfectly coherent with the TEM image is observed beyond the topography contrast in both images. The nature of this contrast can arise from different physical origins. Some studies refer to a strong dependence of the second mode to the Hamaker constant of the material, which should lead to an increased sensitivity of the composition of the surface for this second mode (17, 20, 21). The differential composition should not significantly affect the contrast of the image since in these samples the VLPs are stained with a uranyl acetate. In this case, the dynamics of the excited eigenmodes are mainly sensitive to sample stiffness and related mechanical properties (22, 23). The negative and positive phase shifts observed on the VLP structure, can be explained on the base of a respectively hardening and softening of the VLP surface with respect to the substrate taken as reference. Comparison with TEM image can be used to assign a the brighter area of phase 2 image with a softer surface associated with the VLP membrane, while the darker area should correspond to a hardening of the surface induced by the nuclear protein capsid embedded in the VLP. In this sense, bimodal AFM arises as a powerful tool to investigate complex biological material due to its capability of distinguishing among mechanically different structures of the biological units, with wide applicability in biophysics community [ref E].

To further investigate into the mechanical features, AM-FM Viscoelastic Mapping Mode was applied to analyze the HIV-1 Gag VLPs as shown in Figure 2G-H. In this case, we used the same fundamental resonant frequency f_1=80,21 kHz as in Figure 2B-D, as well as the same parameters for topography imaging in this frequency, that is A_{01} = 92.5 nm and A_{sp} = 71 nm, but the amplitude of the second frequency was kept constant at A_2 = 5.5 nm, and the dissipation resulted from changes in drive energy to keep this amplitude constant were recorded. As the higher resonant frequency was operated in Frequency Modulation, changes in the resonant frequency values were also recorded for this higher excited mode, which are directly proportional to the sample stiffness. The structure observed in this case is again perfectly coherent with the TEM image, but moreover, it provides specific information about the protein capsid content at the capsid of the HIV-1 Gag VLP. Quantitative elastic modulus can be determined from frequency, amplitude, and phase of the two modes following the proper contact mechanics models (23). Young modulus image shown in Figure 2H confirms that the strong contrast observed is in agreement with bimodal AFM image and corresponds to an enhancement of the sample stiffness, which directly correlates the material at the particle core, hence giving direct access to the intramembrane structure. Thus, MF AFM imaging allows for the mapping of the protein capsid inside the lipid membrane that conforms the particle structure, for what it is possible to unequivocally distinguish HIV-1 Gag VLPs deposited on surfaces.

The contrast obtained by MF AFM on HIV-1 Gag VLPs is not dependent of the substrate on which the VLPs are deposited. HIV-1 Gag VLP preparation was deposited on mica substrate and analyzed under ambient conditions by using AM-FM Viscoelastic Mapping Mode. Figure 3A shows the topography distribution over a large area of HIV-1 Gag VLPs on mica substrate. HIV-1 Gag VLP preparations present similar topography as those observed by Faivre-Moskalenco *et al.* and Oropesa *et al.* (14, 15). Moreover, it can be highlighted the large number of VLP-like structures in the sample. Figure 3B shows the topography image and Figure 3C-D the Δf_2 and the Young Modulus images respectively of a single HIV-1 Gag VLP where VLP-like structure, which is characterized by its spherical shape and specific contrast in Δf_2 and Young modulus charts, as observed in the previous negative stained HIV-1 Gag VLP samples deposited on a TEM grid (Figure 2). Moreover, the strong contrast in mechanical properties also arises as a unique

feature that allows to distinguish VLP from other similar contaminating topographical structures or surface roughness. In this sense, similar information is obtained without pre-treating the sample. This confirms the wide applicability of this technique even less resolution is achieved compared to TEM preparation samples.

Figure 2: TEM and AFM imaging of an individual HIV-1 Gag VLP. A) TEM Image B) AFM 3D Topography imaging C) AFM Amplitude and D) Phase Image of the fundamental mode; E) Second Amplitude (A_2) and F) Phase (Φ_2) Images of Bimodal AFM, corresponding to the dynamics of the first excited eigenmode; and G) First excited eigenmode frequency shift (Δf_2) image of AM-FM Viscoelastic mapping mode, and the corresponding calculated H) Young Modulus image

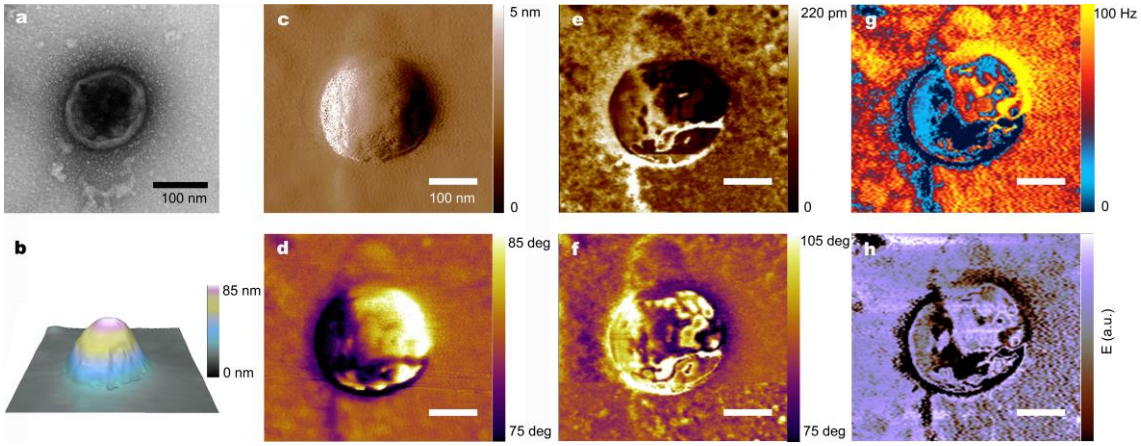

3.4. Discrimination of VLPs and cellular vesicle populations in ambient conditions by AFM

The conspicuous contrast of HIV-1 Gag VLPs obtained by MF AFM prompts to its application as a fast and easy methodology for monitoring VLP production. MF AFM allowed to distinguish VLPs from contaminating cellular vesicles content. Therefore, it is necessary to study the cellular vesicles using the same technique. Characterization of the Mock sample was done by AFM, where isolated vesicles were visualized in EM.

Figure 4 show the AFM images obtained for Mock sample. First significant difference is that no topography evidence is obtained for vesicles, which strongly differs from HIV-1 Gag VLPs structures. The comparison between Figure 3A and Figure 4A, highlight the fact that the structures found in VLP topography chart (Figure 3A) may correspond only to HIV-1 Gag VLPs where the vesicles contamination could not be detected.

Remarkably, a significant contrast of the cellular vesicles with respect to the surroundings is obtained for the $\Phi_1$image (Figure 4B). This contrast is caused by the different interaction of the cantilever tip with the biological sample deposited which have different structural, compositional and/or chemical properties than the mica substrate. The images univocally confirm the observation of the cellular vesicle population present in Mock samples which are mainly composed by lipid membranes, but without the stiff protein capsid content inside the membrane at the core.

Figure 3: Individual VLP deposited on mica substrate. A) AFM topography image of VLPs on mica substrate B) 3D topography image of a single VLP structure. C) Δf2 Imaging of an isolated VLP structure, as obtained by AM-FM Viscolastic mapping mode and D) the corresponding calculated Young Modulus distribution

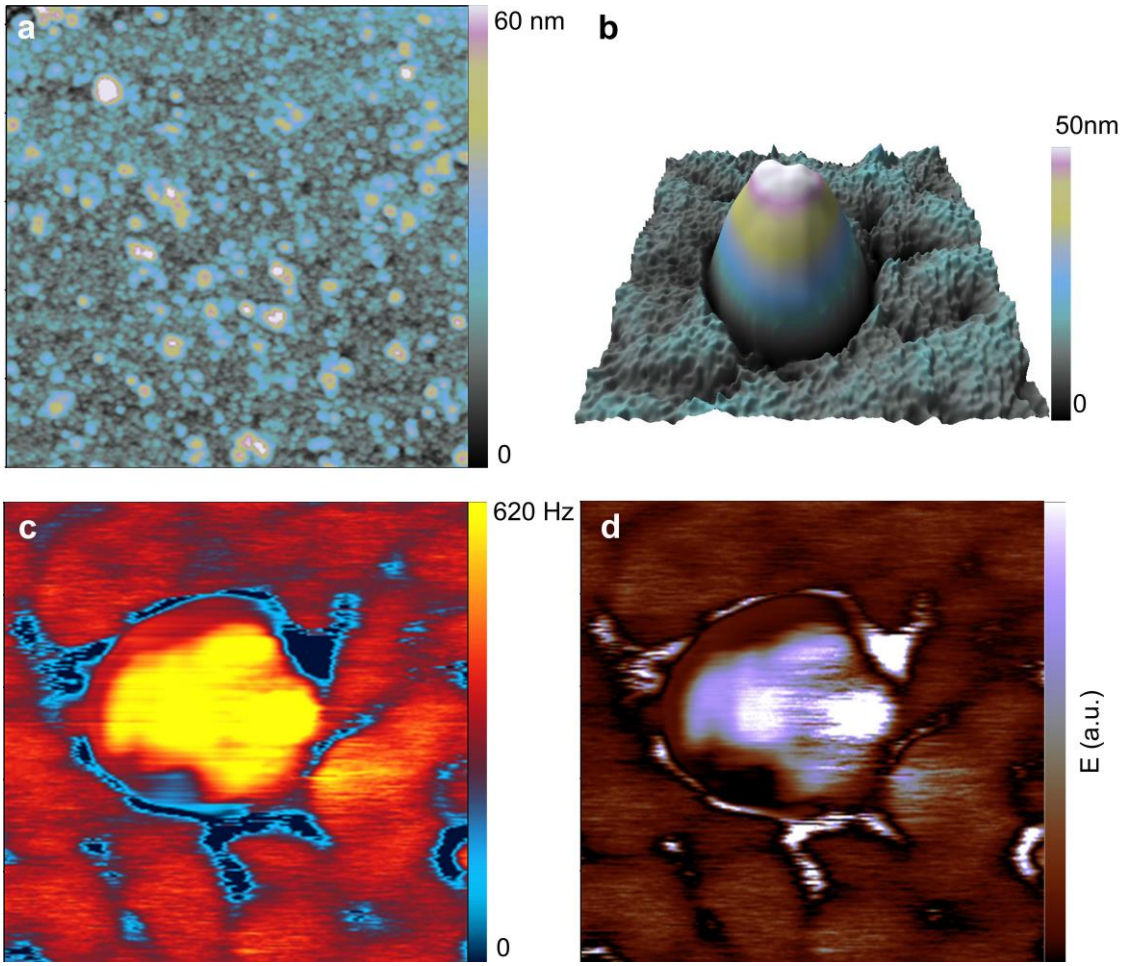
a
60 nm
0
b
50nm
0
c
620 Hz
0
d
E (a.u.)

Figure 4: Mock sample deposited on mica substrate. A) AFM Topography image of empty cellular vesicles deposited on mica substrate and B) corresponding AFM phase image, showing the contrast due to the presence of the vesicles.

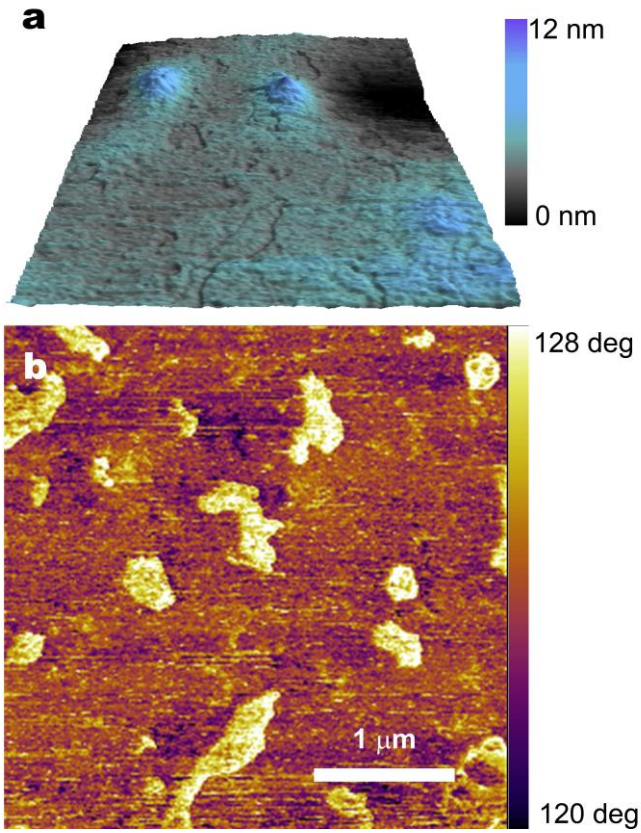

4. CONCLUSIONS

In this work, advanced characterization of enveloped HIV-1 Gag VLPs has been achieved by applying MF AFM. The analysis presents a sphere-like structure without relevant glycoproteins in its surface. Interestingly, novel information regarding the nanomechanical properties of the particle were observed by bimodal and AM-FM Viscoelastic Mapping modes. The enhanced contrast obtained in the surface of the HIV-1 Gag VLPs is related to the Gag self-assembled capsid enveloped by the host lipid membrane. Moreover, the bimodal AFM examination of HIV-1 Gag VLPs and vesicular bodies under ambient conditions enabled its identification and distinction. The application of this advanced MF AFM modes to soft samples unveils new opportunities for the study of capsid proteins composition and nanomechanical qualities of biological materials, with great impact in the biophysics community, and its further use for the development of proper and efficient strategies for the obtention of high quality VLP candidates for vaccination purposes.

5. AUTHOR CONTRIBUTIONS

I.G. and S.G. produced the HIV-1 Gag VLPs candidates, I.G and N.D. performed the experiments and data analysis. I.G, S.G., L.C., F.G. and N.D. wrote the manuscript.

6. ACKNOWLEDGMENTS

The authors wish to thank Dr. Amine Kamen (McGill, Montreal, Canada) for providing the HEK 293 SF-3SF6. The following reagent was obtained through the NIH AIDS reagent Program, Division AIDS, NIAID, NIH: pGag-EGFP (Cat# 11468) from Dr. Merilyn Resh. We would like to thank Dr Albert Verdaguer from ICN2 (Bellaterra, Spain) for providing mica substrate and for its valuable discussions about bimodal AFM. The help of Dr. Pablo Castro from Servei de Microscòpia (UAB, Spain) in the development of electron microscopy analysis is greatly appreciated. This work was supported by the Plan Nacional de Investigación, Ministry of Science and Innovation (MINECO BIO2011-2330), and

projects from the Spanish Ministerio de Economía y Competitividad FIS2013-48668-C2-1-P, and the Generalitat de Catalunya under project 2014 SGR 1216. ICN2 acknowledges support from the Severo Ochoa Program (MINECO, Grant SEV-2013-0295). N.D. wants to acknowledge the Spanish Ministerio de Ciencia e Innovación for a Ramon y Cajal research grant RYC-2010-06365.

7.LITERATURE

1. Organization, W.H. 2015. World AIDS Day. World AIDS Day 2015 Get. to zero. Web 02 Feb: http://www.who.int/.

2. Cohen, Y.Z., and R. Dolin. 2013. Novel HIV vaccine strategies: overview and perspective. Ther. Adv. Vaccines. 1: 99–112.

3. Göttlinger, H.G. 2001. HIV-1 Gag : a Molecular Machine Driving Viral Particle Assembly and Release. Theor. Biol. Biophys. Group, Los Alamos Natl. Lab. Los Alamos, NM, LA-UR 02-2877. 2-28.

4. Kushnir, N., S.J. Streatfield, and V. Yusibov. 2012. Virus-like particles as a highly efficient vaccine platform: Diversity of targets and production systems and advances in clinical development. Vaccine. 31: 58–83.

5. Naskalska, A., and K. Pyrć. 2015. Virus Like Particles as Immunogens and Universal Nanocarriers. Pol. J. Microbiol. 64: 3–13.

6. Noad, R., and P. Roy. 2003. Virus-like particles as immunogens. Trends Microbiol. 11: 438–444.

7. Cervera, L., S. Gutiérrez-Granados, M. Martínez, J. Blanco, F. Gòdia, and M.M. Segura. 2013. Generation of HIV-1 Gag VLPs by transient transfection of HEK 293 suspension cell cultures using an optimized animal-derived component free medium. J. Biotechnol. 166: 152–65.

8. Gutiérrez-Granados, S., L. Cervera, M. de L.M. Segura, J. Wölfel, and F. Gòdia. 2015. Optimized production of HIV-1 virus-like particles by transient transfection in CAP-T cells. Appl. Microbiol. Biotechnol. DOI10.1007: s00253–015–7213–x.

9. Akers, J.C., D. Gonda, R. Kim, B.S. Carter, and C.C. Chen. 2013. Biogenesis of extracellular vesicles (EV): Exosomes, microvesicles, retrovirus-like vesicles, and apoptotic bodies. J. Neurooncol. 113: 1–11.

10. Bess, J.W., R.J. Gorelick, W.J. Bosche, L.E. Henderson, and L.O. Arthur. 1997. Microvesicles are a source of contaminating cellular proteins found in purified HIV-1 preparations. Virology. 230: 134–44.

11. Gluschankof, P., I. Mondor, H.R. Gelderblom, and Q.J. Sattentau. 1997. Cell membrane vesicles are a major contaminant of gradient-enriched human immunodeficiency virus type-1 preparations. Virology. 230: 125–133.

12. Thompson, C.M., E. Petiot, A. Mullick, M.G. Aucoin, O. Henry, and A.A. Kamen. 2015. Critical assessment of influenza VLP production in Sf9 and HEK293 expression systems. BMC Biotechnol. 15: 31.

13. Gutierrez-Granados, S., L. Cervera, F. Godia, J. Carrillo, and M.M. Segura. 2013. Development and validation of a quantitation assay for fluorescently tagged HIV-1 virus-like particles. J. Virol. Methods. 193: 85–95.

14. Oropesa, R., J.R. Ramos, V. Falcón, and A. Felipe. 2013. Characterization of virus-like particles by atomic force microscopy in ambient conditions. Adv. Nat. Sci. Nanosci. Nanotechnol. 4: 025007.

15. Faivre-Moskalenko, C., J. Bernaud, A. Thomas, K. Tartour, Y. Beck, M. Iazykov, J. Danial, M. Lourdin, D. Muriaux, and M. Castelnovo. 2014. RNA control of HIV-1 particle size polydispersity. PLoS One. 9: e83874.

16. Kuznetsov, Y.G., and A. McPherson. 2011. Atomic Force Microscopy in Imaging of Viruses and Virus-Infected Cells. Microbiol. Mol. Biol. Rev. 75: 268–285.

17. Garcia, R., and E.T. Herruzo. 2012. The emergence of multifrequency force microscopy. Nat. Nanotechnol. 7: 217–226.

18. Lozano, J.R., and R. Garcia. 2008. Theory of Multifrequency Atomic Force Microscopy. Phys. Rev. Lett. 100: 076102.

19. Kuznetsov, Y.G., J.G. Victoria, W.E. Robinson, and A. Mcpherson. 2003. Atomic Force Microscopy Investigation of Human Immunodeficiency Virus (HIV) and HIV-Infected Lymphocytes. J. Virol. 77: 11896–909.

20. Martinez, N.F., S. Patil, J.R. Lozano, and R. Garcia. 2006. Enhanced compositional sensitivity in atomic force microscopy by the excitation of the first two flexural modes. Appl. Phys. Lett. 89: 153115.

21. Santos, S., V. Barcons, J. Font, and A. Verdaguer. 2014. Unlocking higher harmonics in atomic force microscopy with gentle interactions. Beilstein J. Nanotechnol. 5: 268–77.

22. Garcia, R., and R. Proksch. 2013. Nanomechanical mapping of soft matter by bimodal force microscopy. Eur. Polym. J. 49: 1897–1906.

23. Proksch, R., and D.G. Yablon. 2012. Loss tangent imaging: Theory and simulations of repulsive-mode tapping atomic force microscopy. Appl. Phys. Lett. 100: 073106.